Number of independent spatial modes in a spherical volume

←Quantum

Quantum optics spatial modes inside a spherical volume

is based on **Quantum optics** a branch of atomic, molecular, and optical physics and quantum chemistry that studies the behavior of photons (individual quanta of light). and refers to the number of simultaneously supportable propagable orthogonal spatial modes in the wavefield confined in a spherical region of radius R with negligible crosstalk. The concept applies equally well in both the classical and quantum channels and deals with electromagnetic waves (light or radio waves), acoustic waves (sound or ultrasonic waves), or de Broglie matter waves. Since the early days of spherical near-field far-field transformations [5][6] a recommendation for the necessary number of polar modes has been given by $N = kr_0 + 10$ [35], k being the wavenumber and r_0 the radius of the minimum sphere. The almost explosive development in computer speed and storage capacity witnessed during the last two decades has made transformations of fields from antennas exceeding thousands of wavelengths feasible, and a closer investigation of the above expression seems to be appropriate.

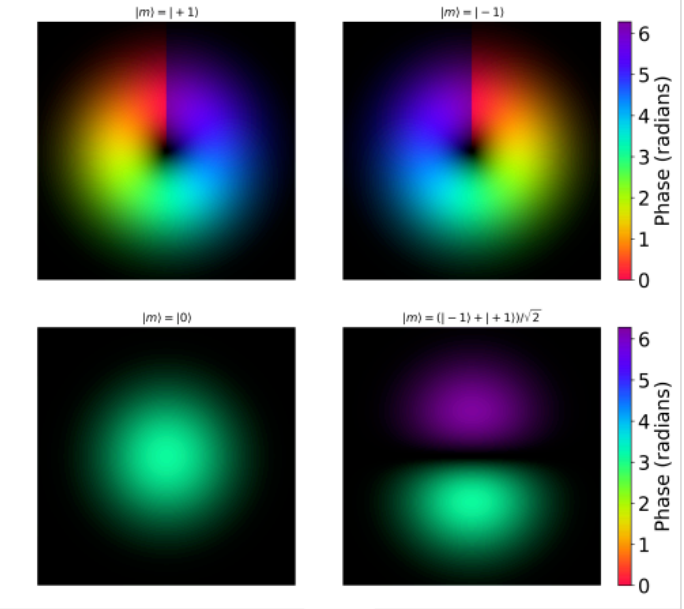

Phase and amplitude plots of several Laguerre–Gaussian modes with different radial index p and azimuthal index ℓ. These form a complete orthogonal basis commonly used to count the number of independent spatial modes ("beams") that can fit inside a spherical or cylindrical volume of radius R.

An improved expression for the number of modes, N, related to the antenna size and the required accuracy will be developed. The impact of truncation of the modal expansion at a given level will be illustrated. This is especially important for measurements where noise is present, or where there is undesirable scattering from objects.

Turchin and Tseytlin [7] have stated that $N = n_o + 3/(1 - (n_o/(kr_o))^3)$ but neither a justification nor

Modes, Spherical Expansion, Spherical Modes, Spherical Near Field, Spherical Waves. Antenna measurement, echo suppression, spherical wave expansion, vector addition theorem[32], mode filtering.

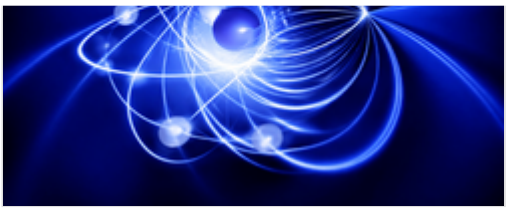

Artistic impression of an atom 2d

Modes

Every beam corresponds to a different orthogonal mode in the spatial structure of the electromagnetic field (for example, Laguerre–Gaussian modes, Hermite–Gaussian modes, or spherical-harmonic modes). The number of such modes in principle depends upon the size of the accessible phase space defined in the sphere and finally upon the diffraction limit contained in the wavelength λ.[1][3] This applies in many fields. For quantum optics and quantum information research, this determines the maximum dimensionality of quantum entanglement in the spatial mode and the quantum capacity of free-space quantum communication channels.[2] For classical free-space optical communication links, the same counting gives the ultimate (hole-burning-free) upper bound on the number of independent spatial channels, the diffraction-limited number of spatial degrees of freedom (a three-dimensional analogue of the familiar A/λ^2 limit for planar apertures).[1]

Artistic visualization of independent spatial modes (spherical harmonics) inside a spherical volume..

Applications

For phased arrays in radar or radio astronomy applications, this defines the number of independently beam-steerable or spatially resolvable beams or channels. For medical ultrasonic imaging or sonar applications, this closely-related idea defines the number of independently addressable focal areas or image pixels. Theoretically, in the latest volumetric or five-dimensional optical information recording technologies, this determines the overall data packing density if all possible spatial and polarization freedoms are utilized.[1] Since the same counting in the phase-space argument holds equally for classical waves and quantum states consisting of one or few photons, this limit turns out to be universal.[2][1][3][A][4]

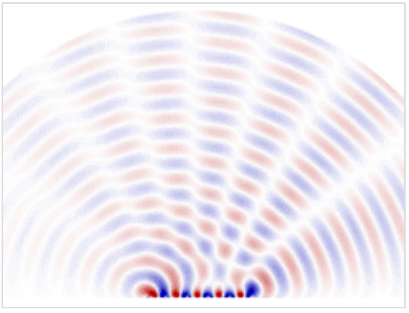

Animation showing the radiation pattern

The theorem is central to post-processing techniques for echo and reflection suppression in antenna measurements. By offsetting the antenna under test (AUT) and translating modes back to the origin, direct and scattered signals separate in modal space, allowing filtering of unwanted higher-order modes.

It is particularly valuable in spherical near-field (SNF) measurements, probe compensation, and RCS analysis.

displacements that can be smaller or larger than the maximum radial extent of the antenna.
- Crucially, this article shows how the all-important vector addition coefficients can be obtained from the scalar coefficients for which efficient, accurate, and precise recurrence relations exist, which greatly reduces the computational effort required, which would otherwise likely render the technique impractical.

What is the implication of the main finding?

- The technique presented provides the first-ever algorithm for applying mode-filteringbased reflection suppression without the need to first transform to the asymptotic far-field, yielding a significant generalization of the algorithm;
- The new algorithm represents a notable development as it is rigorous and general, incorporating both reactive and propagating components, thereby making the processing applicable to a wider range of problems than has previously been the case.

Abstract Monochromatic mode-filtering-based scattering suppression techniques have been shown to be applicable to all commonly used forms of far- and near-field antenna and RCS measurement techniques. Traditionally, the frequency-domain mode-filtering technique takes a far-field pattern, either measured directly or obtained using a suitable near-field to far-field transformation, as its starting point. The measurement is required to be conducted such that the antenna under test (AUT) is positioned offset from the origin of the measurement coordinate system. This physical offset introduces a phase taper across the AUT pattern and results in far greater interference occurring between the direct and indirect parasitically coupled spurious scattered signals. The method is very general and can be applied to all forms of near- or far-field measurements. However, for the case of a spherical near-field measurement (SNF) approach, it is somewhat cumbersome and tedious as first we must perform a probe-corrected spherical near-field to far-field transformation, which itself involves the computation of a complete set of spherical mode coefficients, and then after the displacement has been applied to the far-electric-fields, a second spherical wave expansion

History

The fundamental limit imposed by a finite volume on the number of independent communication channels was first analysed in optics during the 1960s and 1970s.[36][37] These works showed that the number of spatial degrees of freedom of a field confined to a region of radius R scales as $(2\pi R/\lambda)^2$ in two dimensions and $(2\pi R/\lambda)^3$ in three dimensions.

In 2000, David A. B. Miller used this precise expression for the number of orthogonal spatial channels that can be supported between two spherical volumes in free space, formula $N \approx (kR)^3 / (3\pi^2)$ when both polarisations are included.[1]This result has become the standard reference for the maximum number of “beams in a sphere”.

In 2004 Frank Jensen published "On the number of modes in spherical wave expansions"[35] describing polar modes and improved expression for the number of modes

Since the mid-2010s, the same spatial-mode counting argument has been widely applied in high-dimensional quantum optics, where approximately $(kR)^3$ modes (orbital-angular-momentum, Laguerre–Gaussian, or pixel bases) are used as independent quantum channels.[2][3] When finite bandwidth Δf and observation time t are taken into account, the total number of independent spatio-temporal channels is

In 2023 Marc Dinix et al. published Generalized Vector Addition Thorem for displacements[32] that can be smaller or larger than the maximum radial extent of the object[10]

David A. B. Miller

Modern vector addition coefficients

- Unlike other perhaps better-known techniques, the generalized vector addition theorem can be successfully utilized to perform object position translations in any direction, and for displacements that can be smaller or larger than the maximum radial extent of the antenna;
- Crucially, this article shows how the all-important vector addition coefficients can be obtained from the scalar coefficients for which efficient, accurate, and precise recurrence relations exist, which greatly reduces the computational effort required, which would otherwise likely render the technique impractical.

Implications

- The technique provides the first-ever algorithm for applying mode-filtering-based reflection suppression without the need to first transform to the asymptotic far-field, yielding a significant generalization of the algorithm;
- The new algorithm represents a notable development as it is rigorous and general, incorporating both reactive and propagating components, thereby making the processing applicable to a wider range of problems than has previously been the case.

The conventional vector addition theorem is written in a compact notation. Then a new and succinct derivation of the vector addition theorem is as close to the derivation of the scalar addition theorem. Newly derived expressions in this new derivation are used to diagonalize the vector addition theorem[32]. The diagonal form of the vector addition theorem is important in the design of fast algorithms for computational wave physics such as computational electromagnetics and computational acoustics. Monochromatic mode-filtering-based scattering suppression techniques have been shown to be applicable to all commonly used forms of far- and near-field antenna and RCS measurement techniques. Traditionally, the frequency-domain mode-filtering technique takes a far-field pattern, either measured directly or obtained using a suitable near-field to far-field transformation, as its starting point. The measurement is required to be conducted such that the antenna under test (AUT) is positioned offset from the origin of the measurement coordinate system.

While the vector addition theorem required for the spherical near-field to far-field transformation (SNFFFT) algorithm has been described in detail in the open literature, its implementation has been limited to the case of impinging waves and positive z-directed translations where the magnitude of the displacement is necessarily larger than the minimum sphere radius (MRE).

Although many scattering suppression methods have been proposed, with examples including time-gating (both hardware and software), spatial filtering, RF background subtraction, parametric repeat measurements, and waveform correlation, it is only during the past two decades that the use of mode orthogonalization and filtering-based postprocessing techniques have become widely deployed in industry and academia to identify and subsequently extract measurement artifacts arising from parasitically coupled spurious scattered fields in antenna pattern and radar cross-section (RCS) measurements [12][13][14][15][16][17]. These have been used very successfully to greatly improve the facility-level uncertainty budget [18] and have gradually become available for use with all commonly encountered forms of near-field and far-field antenna range measurements. These single-frequency mode-filtering-based approaches have been extended to admit the possibility of processing data that are sampled on irregular grids [17] and, more recently, have been extended to take advantage of sparse sampling compressive sensing techniques [19][20].

Generalized vector addition theorem

The volume element in spherical coordinates is crucial for deriving the orthogonality relations of spherical harmonics and vector spherical wave functions, as integrals over the sphere involve the Jacobian factor $\rho^2 \sin \varphi$.

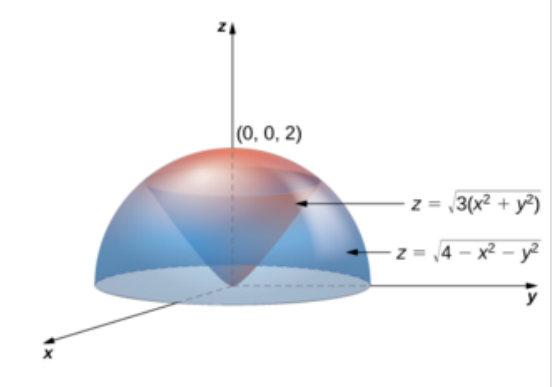

The volume element in spherical coordinates is $\Delta V \approx \rho^2 \sin \varphi \, \Delta\rho \, \Delta\varphi \, \Delta\theta$, leading to $dV = \rho^2 \sin \varphi \, d\rho \, d\varphi \, d\theta$.

This Jacobian ensures proper normalization of the modes over spherical surfaces, forming the basis for multipole expansions used in the translation addition theorem.

A generalized form of the theorem, valid for arbitrary translation directions and distances (including those smaller or larger than the antenna's minimum radial extent), was developed by Marc Dirix, Stuart F. Gregson, and Rostyslav F. Dubrovka in 2025.[38]

This generalization enables direct translation of spherical mode coefficients without intermediate far-field transformations, preserving both propagating and evanescent modes.

It supports translations in any direction and for any displacement magnitude, overcoming limitations of classical formulations that required specific conditions (e.g., translation along the z-axis or far-field approximations).

The approach uses efficient recurrence relations to compute translation coefficients from scalar wave expansions, reducing computational complexity.

Key applications include advanced spherical near-field antenna measurements, where it facilitates mode-filtering-based reflection suppression in environments contaminated by parasitic scattering.

Section 1

The core translation equation (Eq. 1) is:

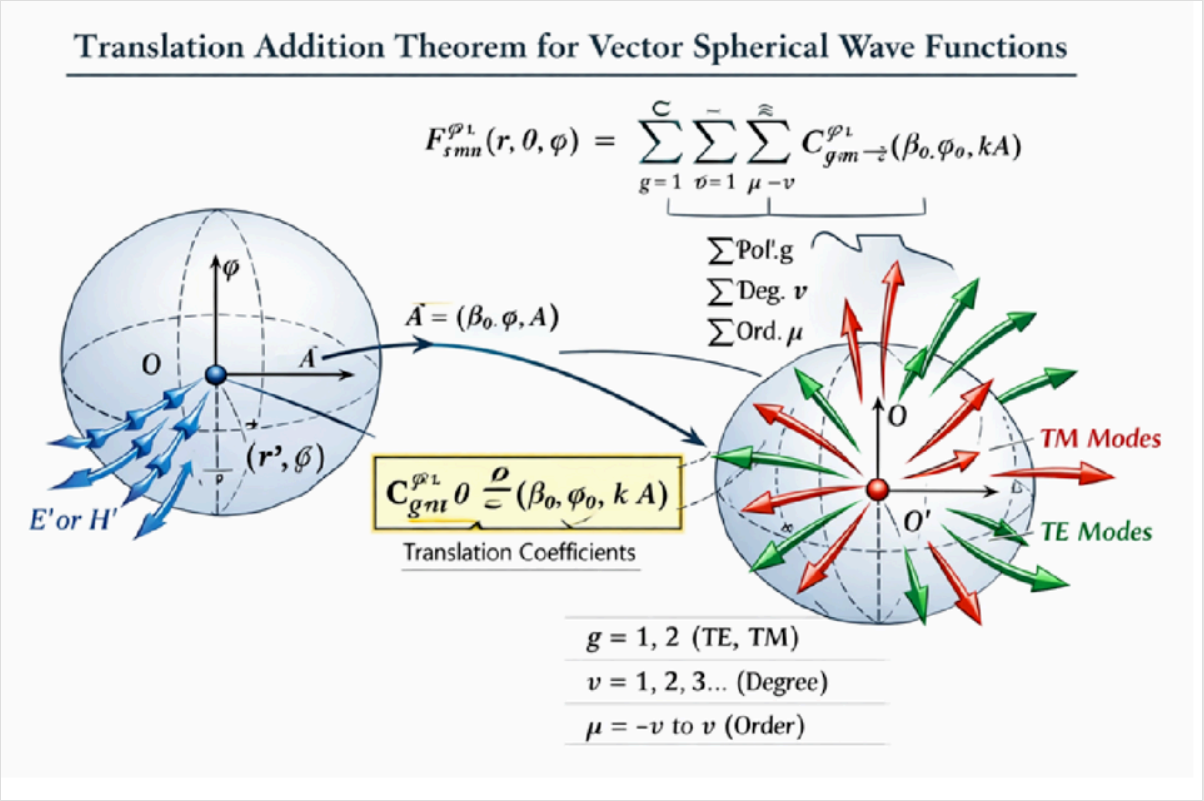

Translation Addition Theorem for Vector Spherical Wave Functions

$$F_{smn}^{(-c)}(r,\theta,\phi) = \sum_{g=1}^{2}\sum_{\nu=1}^{\infty}\sum_{\mu=-\nu}^{\nu} C_{g\mu 0}^{smn(-c)}(\beta_0,\phi_0,kA)\, F_{\sigma(g)\mu\nu}^{(-3)}(r',\theta',\phi') \text{ (Eq. 1)}$$

where:

- $F_{smn}^{(-c)}$ are vector spherical wave functions (s=1,2 for TE/TM modes),
- superscript $(-c)$ denotes radial dependence,
- primed coordinates are translated by distance A along the z-axis (general direction via angles β_0, ϕ_0),
- C are translation coefficients derived efficiently from scalar recurrence relations.

This form removes previous limitations (e.g., requiring translation distance > minimum radial extent) and affects only the far-field phase when translation is inside the minimum sphere, generalizing the phase shift $e^{jk\hat{r}\cdot\mathbf{A}}$. The translation coefficients are defined as [24] and can further be expressed as

$$C_{\sigma\mu\nu}^{smn}(\theta_0,\varphi_0,kA) = \alpha\left[\delta_{s\sigma}A_{\mu\nu}^{mn}(\theta_0,\varphi_0,kA) + \delta_{3-s,\sigma}B_{\mu\nu}^{mn}(\theta_0,\varphi_0,kA)\right] \text{(Eq.2)}$$

(A1) of [24]. For the present work, however, the translation coefficients $A_{\sigma\mu\nu}$ (A1) and $B_{\sigma\mu\nu}$ (A1) are based on the spherical wave functions [25], while the SWE utilized to attain the spherical mode coefficients employs the normalization proposed in [23][26]. Thus, the requisite correction factor for the normalization employed here can be expressed as

$$\alpha = \sqrt{\frac{\nu(\nu+1)}{n(n+1)}} \quad \{\textbf{Eq.3}\}$$

with

$$A_{\mu\nu}^{mn}(\theta_0, \varphi_0, kA) = \sum_{p=|n-\nu|}^{n+\nu} i^{-p}[n(n+1)+\nu(\nu+1)-p(p+1)]a(m,n,-\mu,\nu,p) z_p^{(c)}(kA) P_p^{m-\mu}(\cos\theta_0) e^{i(m-\mu)\varphi_0}$$

$\{\textbf{Eq.4}\}$

and

$$B_{\mu\nu}^{mn}(\theta_0, \varphi_0, kA) = \sum_{p=|n-\nu|}^{n+\nu} i^{-p}[n(n+1)+\nu(\nu+1)-p(p+1)]b(m,n,-\mu,\nu,p-1) z_p^{(c)}(kA) P_p^{m-\mu}(\cos\theta_0) e^{i(m-\mu)\varphi_0}$$

$\{\textbf{Eq.5}\}$

where the linearization coefficient *b* is

$$b(m,n,-\mu,\nu,p) = \frac{2p+1}{2p-1}\Big[(\nu-\mu)(\nu+\mu+1)\,a(m,n,-\mu-1,\nu,p) - (p-m+\mu)(p-m+\mu+1)\,a(m,n,-\mu+1,\nu,p) + 2\mu(p-m+\mu)\,a(m,n,-\mu,\nu,p)\Big] \quad \{\textbf{Eq.6}\}$$

Here, a(m, n, −μ, ν, p)'s are the linearization coefficients, which can be expressed in terms of Wigner 3-j symbols [25], and $z_p^{(c)}$ is the spherical radial function of order p and type (c). Furthermore, $P_p^{m-\mu}(\cos\theta_0)$ denotes the associated Legendre function of degree p and order (m −μ). However, given the number of factorials required, these turn out to be enormously computationally expensive to calculate directly. Fortunately, an alternative strategy may be harnessed involving the computation of these coefficients by means of efficient, stable recurrence relations [24]. Recurrence relations greatly reduce the computational complexity of calculating the coefficients, with this becoming increasingly important as the number of coefficients increases. This is especially crucial as the highest-order coefficient depends upon the frequency, minimum sphere radius, and the size of the translation. Once the scalar coefficients have been obtained, these can then be used to derive the vector addition coefficients.

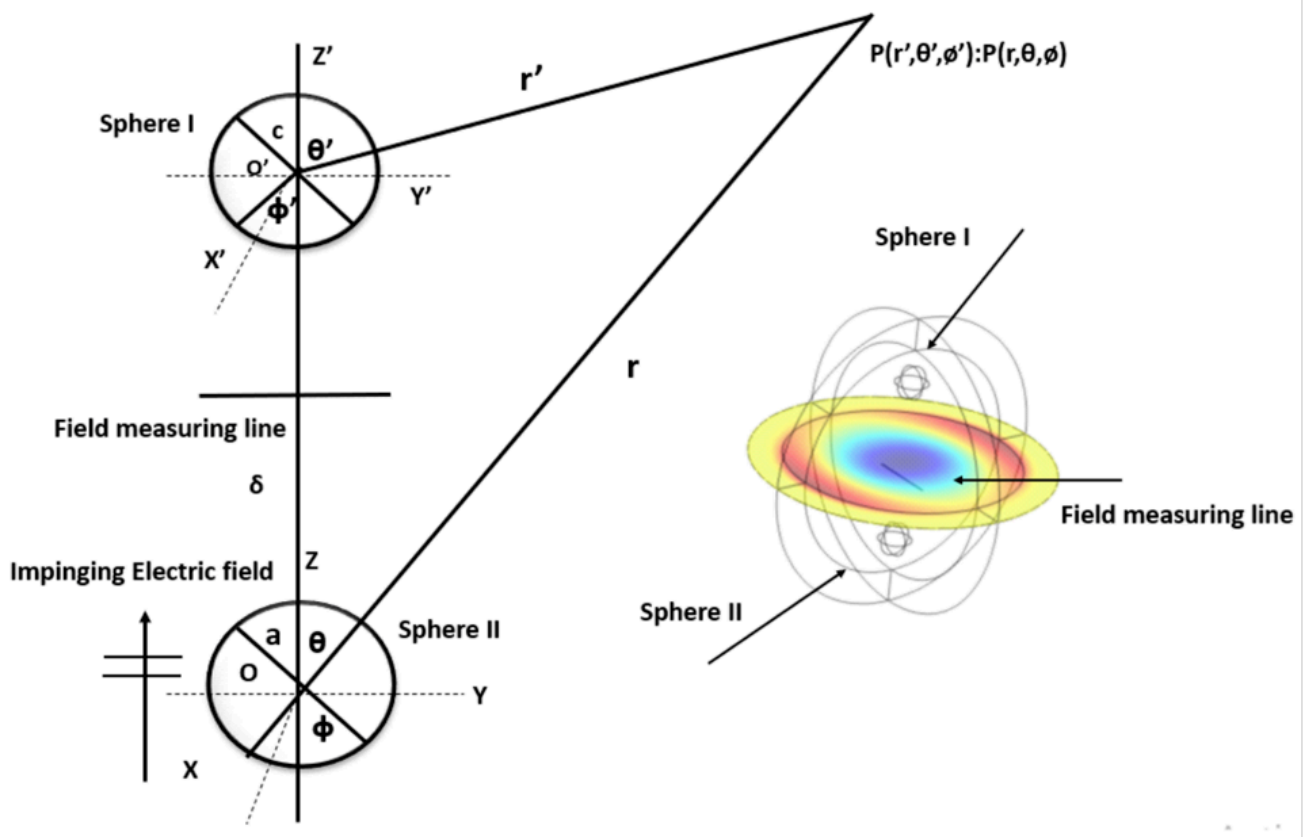

Geometry of two PEC spheres separated by δ along the z-axis, illustrating the translation addition theorem for vector spherical waves.

$$
\begin{aligned}
A_{\mu\nu}^{mn}(\theta_0,\phi_0,kA) &= \beta_{\mu\nu}^{mn}(\theta_0,\phi_0,kA) \\
&+ kA\sin\theta_0\, e^{-i\phi_0}\,\frac{1}{2(\nu+1)}\sqrt{\frac{(\nu-\mu+2)(\nu-\mu+1)}{(2\nu+1)(2\nu+3)}}\,\beta_{\mu-1,\nu+1}^{mn}(\theta_0,\phi_0,kA) \\
&- kA\sin\theta_0\, e^{-i\phi_0}\,\frac{1}{2\nu}\sqrt{\frac{(\nu+\mu-1)(\nu+\mu)}{(2\nu-1)(2\nu+1)}}\,\beta_{\mu-1,\nu-1}^{mn}(\theta_0,\phi_0,kA) \\
&- kA\sin\theta_0\, e^{i\phi_0}\,\frac{1}{2(\nu+1)}\sqrt{\frac{(\nu+\mu+2)(\nu+\mu+1)}{(2\nu+1)(2\nu+3)}}\,\beta_{\mu+1,\nu+1}^{mn}(\theta_0,\phi_0,kA) \\
&+ kA\sin\theta_0\, e^{i\phi_0}\,\frac{1}{2\nu}\sqrt{\frac{(\nu-\mu)(\nu-\mu-1)}{(2\nu-1)(2\nu+1)}}\,\beta_{\mu+1,\nu-1}^{mn}(\theta_0,\phi_0,kA) \\
&+ kA\sin\theta_0\,\frac{1}{\nu+1}\sqrt{\frac{(\nu+\mu+1)(\nu-\mu+1)}{(2\nu+1)(2\nu+3)}}\,\beta_{\mu,\nu+1}^{mn}(\theta_0,\phi_0,kA) \\
&+ kA\sin\theta_0\,\frac{1}{\nu}\sqrt{\frac{(\nu+\mu)(\nu-\mu)}{(2\nu-1)(2\nu+1)}}\,\beta_{\mu,\nu-1}^{mn}(\theta_0,\phi_0,kA)\ \{\text{Eq.7}\}
\end{aligned}
$$

and

$$+\sqrt{(\nu+\mu)(\nu-\mu+1)}\,e^{-i\phi_0}\,\beta^{mn}_{\mu-1,\nu}(\theta_0,\phi_0,kA)\Big]$$ (**Eq.8**)

Here, (**Eq. 7**) and (**Eq. 8**) refer to the calculation of the scalar translation matrix, which is in the form of $\beta^{mn}_{\mu\nu}(\theta_0,\phi_0,kA)$, for which recurrence relations also exist and are developed in [27]. Here, the starting values for n = 0, m = 0, i.e., $\beta^{00}_{\nu\mu}(\theta_0,\phi_0,kA)$ can be easily derived from the scalar wave equation using

$$\beta^{00}_{\nu\mu}(\theta_0,\phi_0,kA)=(-1)^{\mu+\nu}\sqrt{4\pi}\,Y_{\nu,-\mu}(\theta_0,\phi_0)\,z^{(c)}_n(kA)$$ (**Eq.9**)

Here, \(z^{(c)}_n\) is the spherical radial function of order n and type (c).

$$Y_{n,m}(\theta_0,\phi_0)=(-1)^m\sqrt{\frac{(n-m)!(2n+1)}{(n+m)!4\pi}}P_n^{|m|}(\cos\theta_0)e^{im\phi_0}$$ (**Eq10**)

$P_n^{|m|}(\cos\theta)$ is the associated Legendre function. This calculation also makes use of the standard relation $Y_{n,-m}(\theta_0,\phi_0)=(-1)^m Y^*_{n,m}(\theta_0,\phi_0)$ [27]. Then, $\beta^{mn}_{\mu\nu}$ may be expanded using the relation where \(P_n^{|m|}(\cos\theta)\) is the associated Legendre function. This calculation also makes use of the standard relation $Y_{n,-m}(\theta_0,\phi_0)=(-1)^m Y^*_{n,m}(\theta_0,\phi_0)$ [27]. Then, $\beta^{mn}_{\mu\nu}$ may be expanded using the relation

$$b^+_{nn}\beta^{n+1,n+1}_{\mu\nu}=b^+_{\nu-1,\mu-1}\beta^{nn}_{\mu-1,\nu-1}+b^-_{\nu+1,\mu-1}\beta^{nn}_{\mu-1,\nu+1}$$ (**Eq.11**)

where

$$b^+_{nm}=\sqrt{\frac{(n-m)(n-m-1)}{(2n+1)(2n-1)}}$$ (**Eq.12**)

and

$$b^-_{nm}=\sqrt{\frac{(n+m+2)(n+m+1)}{(2n+1)(2n+3)}}$$ (**Eq.13**)

Section 3

The recurrence relation

for $\beta^{n+1,m}_{\mu\nu}$ is derived from the $\beta^{nn}_{\mu\nu}$ values, where the starting points are *m* = *n* so that the requisite recurrence relations are

$$a^+_{nm}\beta^{n+1,m}_{\mu\nu}=-a^-_{nm}\beta^{n-1,m}_{\mu\nu}+a^+_{\nu-1,\mu}\beta^{n,\nu-1}_{\mu\nu}+a^-_{\nu+1,\mu}\beta^{n,\nu+1}_{\mu\nu}$$ (**Eq.14**)

where

and

$$a_{nm}^{-} = \sqrt{\frac{(n+m)(n-m)}{(2n+1)(2n-1)}}$$ (**Eq.16**)

Lastly, $\beta_{\mu\nu}^{n,-m}$ is derived from $\beta_{\mu\nu}^{n,m}$ using $\beta_{\nu\mu}^{n,-m} = (-1)^{\mu+m}\beta_{\nu,-\mu}^{nm}$ (**Eq.17**)

Thus, using (**Eq.1**), a translation can be applied in any direction and in either sense, where the displacement is defined as r = θ0 ˆθ + φ0 ˆφ + kAˆr, and where the magnitude of the displacement |r| can be larger or smaller than the minimum sphere radius.

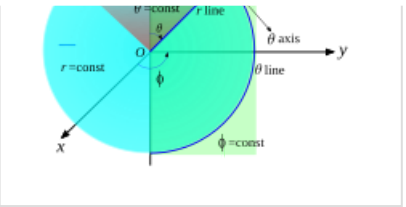

Elements of spherical coordinates: constant-r surfaces (spheres), constant-θ surfaces (cones), constant-φ surfaces (half-planes), coordinate lines, and axes.

Section 4

The memory consumption

of the final translation matrix depends on the number of input and output modes considered. If the AUT at the input is displaced, the occupied MRE is expected to be larger than the AUT itself, which, after translation back to the origin, is reduced. The size of the translation matrix can be written as follows, assuming for each point P a double-precision complex number:

$$P = J_{in} \cdot J_{out} = 2N_{in}(N_{in}+2) \cdot 2N_{out}(N_{out}+2)$$ (**Eq.18**)

with

$$N = \frac{2\pi a}{\lambda},$$ (**Eq.19**)

where a is the MRE, and λ is the wavelength.

For the pre-calculation of $\beta_{\mu,\nu}^{mn}$, however, a matrix of the following size is required as well, which is about half the size of the translation matrix:

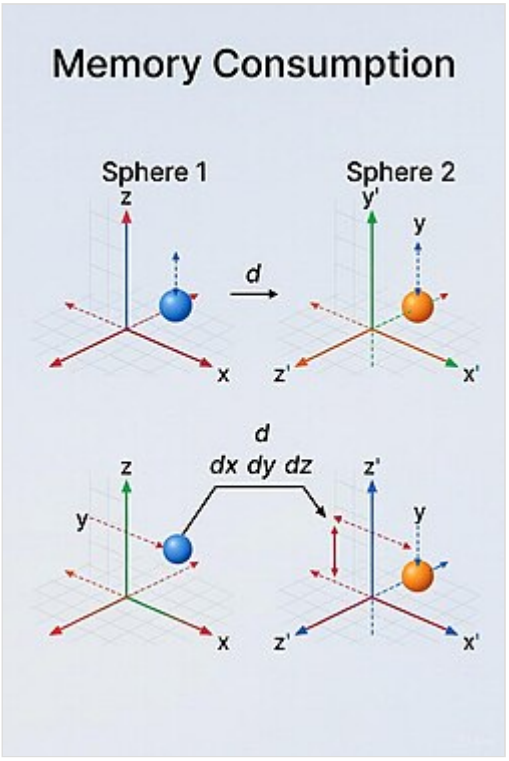

Two translated conducting spheres with glowing electromagnetic fields, illustrating memory consumption in multiple scattering computations.

$$P = ((N_{in}+N_{out})(N_{in}+N_{out}+2)+1) \cdot (N_{out}(N_{out}+2)+1)$$ (**Eq.20**)

In principle, there is no practical numerical limitation to the maximum number of N-modes that can be used with the recursive formulations to determine the translation matrix. However, the direct calculation of the Legendre polynomials currently utilized has a higher-order limit of approximately N = 85, although

To verify this, a simulated far-field pattern of a standard gain horn (SGH) centered at the origin is offset by applying a phase taper:

$$w_{\text{offset}}(\theta,\phi) = w_0(\theta,\phi)\, e^{jk\cos\theta\,\text{Offset}} \quad \{\textbf{Eq.21}\}$$

where:

- $w_0(\theta,\phi)$: Original far-field pattern centered at the origin,
- $e^{jk\cos\theta\,\text{Offset}}$: Phase taper introduced by displacing the antenna along the positive z-axis by distance *Offset*,
- $k = 2\pi/\lambda$: Wavenumber.

The offset pattern is then expanded into spherical modes with increased truncation to represent the larger enclosing sphere, translated back using the generalized theorem, filtered if needed, and compared to the original.

Results show excellent agreement (better than numerical precision), confirming no limitation for large offsets when modes are extended accordingly.

Key contributions from Dirix et al. (2025)

- Successful application to translations in any direction and for any displacement magnitude relative to the antenna's radial extent.
- Efficient computation of vector coefficients from scalar coefficients using precise recurrence relations, making the method practical.
- Direct integration into spherical near-field transformation chains, avoiding intermediate far-field transforms and preserving evanescent modes.
- Enables first-ever mode-filtering-based reflection suppression directly on spherical mode coefficients.

The spherical waves

Field variations in φ are limited by the order M and field variations in θ are limited by the degree N . For the general case $M = N$ and the total number of modes is $2NN(+2)$. For objects with some rotational symmetry around the -axis we may have MN. An empirical value for N is $N = kr_o + n_1$ The electric field $\mathbf{E}(\mathbf{r},\theta,\phi) = \sum_{n=1}^{N}\sum_{m=-n}^{n} Q_{smn} F_{smn}(\mathbf{r},\theta,\phi)$radiated from the primed system

$$\vec{F}^{(c=3)}_{smn}(r,\theta,\phi) = \sum_{\sigma=1}^{2}\sum_{\nu=1}^{\infty}\sum_{\mu=-\nu}^{\nu} C^{(c=1)}_{smn\sigma\mu\nu}(\theta_0,\phi_0,kA)\,\vec{F}^{(c=3)}_{\sigma\mu\nu}(r',\theta',\phi') \quad \{\textbf{Eq.23}\}$$

Here, a source of limited extent can be expressed as a weighted sum of spherical waves.[9]

The fundamental diffraction limit is

$$N \approx 2 \times \frac{(kR)^3}{3\pi^2} \approx 0.068 \left(\frac{2\pi R}{\lambda} \right)^3$$

independent spatial modes (including both polarisation states), where $k = \frac{2\pi}{\lambda}$ is the wavenumber.[1][3]

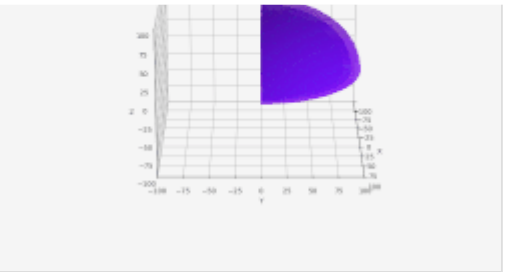

Click for animation.
Concentric spherical shells with rainbow coloring, illustrating nested spherical wave fronts in a 3D rotating view.

The formula above is for vacuum (refractive index $n = 1$). In a dielectric medium with refractive index $n > 1$, the effective wavenumber inside the medium is $n\,k$, so the number of modes becomes:

$$N \approx 2 \times \frac{(nkR)^3}{3\pi^2} \approx 0.068 \left(\frac{2\pi nR}{\lambda} \right)^3$$

In the example calculation (50 μm sphere at 800 nm), an effective refractive index $n \approx 1.5$ (typical for fused silica) is implicitly used, giving $N \approx 2.8 \times 10^7$.

With finite bandwidth Δf and observation time t, the total number of independent spatio-temporal channels becomes

$$N_{\text{total}} \approx N \times \Delta f \times t.$$[3]

Quantum-mechanical limit

A **quantum limit** in physics is a limit on measurement accuracy at quantum scales.[39]

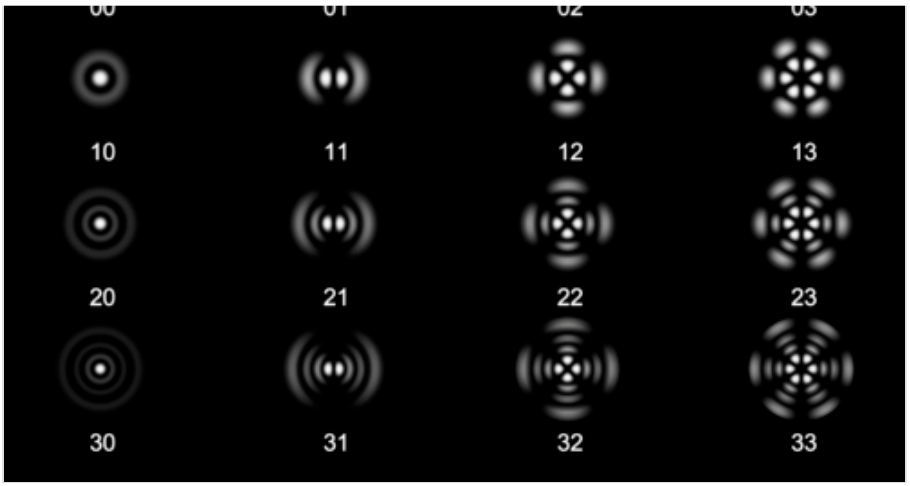

Intensity profiles of Laguerre–Gaussian modes

Artistic visualization of independent spatial modes (spherical harmonics) inside a spherical volume, with rainbow-colored symmetric wave patterns and cosmic background.

Per polarisation:

$$N_{\text{per pol}} \approx \frac{(kR)^3}{3\pi^2}$$

including both polarisations:

$$N \approx 2 \times \frac{(kR)^3}{3\pi^2} \approx 0.068 \left(\frac{2\pi R}{\lambda} \right)^3 .$$ [1][3][40][2] [C]

Classical beam packing

For non-diffracting beams of diameter d, geometric packing gives a crude (and irrelevant) upper bound $N \lesssim (2R/d)^3$.[41][D]

Including time and bandwidth

$$N_{\text{total}} \approx N \times (\Delta f \cdot t)$$[42][E]

Example calculation (50 μm sphere, near-infrared light)

- R = 50 μm, λ = 800 nm → $kR \approx 393$
- $N \approx 2.8 \times 10^7$
- Δf = 10 THz, t = 1 s → $\Delta f \cdot t = 10^{13}$
- $N_{\text{total}} \approx 2.8 \times 10^{20}$

Detailed Mode Number and Time-Bandwidth Product Calculation
kR ≈ 393:
With radius R = 50 μm = 5×10^{-5} m and wavelength λ = 800 nm = 8×10^{-7} m,

wavelength in the sphere's volume, using the formula derived from the photonic density of states (Weyl law) for a large cavity:

$N \approx (8\pi\ n^3\ V)/(3\ \lambda^3)$, where $V = (4/3)\pi\ R^3 \approx 5.24 \times 10^{-13}\ m^3$ is the volume and n accounts for the dielectric.

Without n (vacuum), $N \approx 8.57 \times 10^6$. For n ≈ 1.5 (common approximation for silica), $n^3 = 3.375$, so $N \approx 2.89 \times 10^7$.

For n ≈ 1.453 (precise value for fused silica at 800 nm), $n^3 \approx 3.07$, so $N \approx 2.63 \times 10^7$.

The given 2.8×10^7 is a reasonable approximation, likely using n ≈ 1.5 and rounding.

$\Delta f \cdot t = 10^{13}$:With bandwidth $\Delta f = 10$ THz $= 10^{13}$ Hz and observation time t = 1 s,

$\Delta f \cdot t = 10^{13} \times 1 = 10^{13}$. This is the time-bandwidth product, representing the number of independent temporal modes. This matches.

$N_{total} \approx 2.8 \times 10^{20}$: $N_{total} = N \times (\Delta f \cdot t) \approx 2.8 \times 10^7 \times 10^{13} = 2.8 \times 10^{20}$. This multiplication is exact and represents the total degrees of freedom (spatial modes × temporal modes) for signals or photons in the system.

The slight discrepancy in N (2.8×10^7 vs. calculated $2.6–2.9 \times 10^7$) is typical for approximations in n or constants in such models.[F]

Bekenstein bound limits from quantum gravity

The Bekenstein entropy/information bound

According to the universal entropy bound, the entropy (and hence information capacity) of a complete weakly self-gravitating physical system can be bounded exclusively in terms of its circumscribing radius and total gravitating energy. The bound's correctness is supported by explicit statistical calculations of entropy, gedanken experiments involving the generalized second law, and Bousso's covariant holographic bound [34]. On the other hand, it is not always obvious in a particular example how the system avoids having too many states for given energy, and hence violating the bound. We analyze in detail several purported counterexamples of this type (involving systems made of massive particles, systems at low temperature, systems with high degeneracy of the lowest excited states, systems with degenerate ground states, or involving a particle spectrum with proliferation of nearly massless species), and exhibit in each case the mechanism behind the bound's efficacy.

Information theory and the question of storage capacity

Information theory started as a theory of communication transport of information. The developers of communication channel capacity theorems paid little attention to the akin question of information storage capacity.

In essence such question boils down to a more physically sounding one: what are the limitations on the magnitude of the entropy of a system characterized by general parameters such as size, energy, mass, ...?

In 1981 Bekenstein proposed[33] that the entropy of a complete physical system in asymptotically flat $D = 4$ spacetime, whose total mass-energy is E, and which fits inside a sphere of radius R, is necessarily bounded from above:

bearing object is deposited at a black hole's horizon with the least possible energy; a violation of the generalized second law seems to occur unless the said bound applies to the object.[33]

The tenor of the argument is that E is to be interpreted as the gravitating energy of the system; this prescription disposes of any ambiguity that would arise if we attempted to redefine the zero of energy.

Quantum wavefunctions in spheres

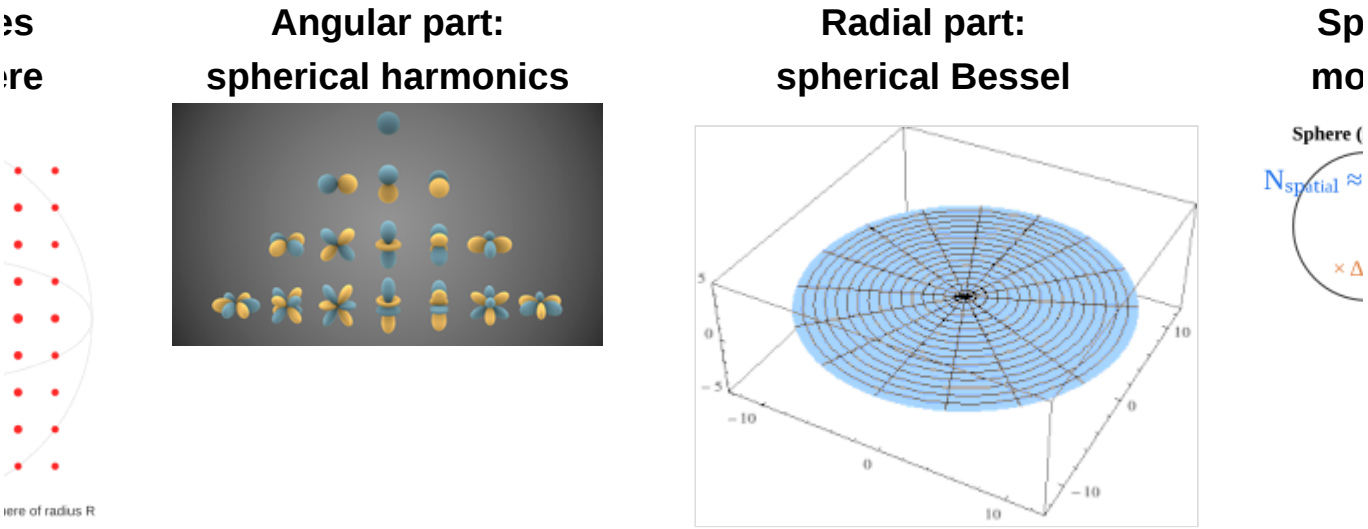

Bessel functions describe the radial part of vibrations of a circular membrane.

Spherical harmonics and Bessel functions are the natural solutions of the Helmholtz or Schrödinger equation (these functions form a complete orthogonal set for the spatial modes in the sphere).

See also

- Quantum
- Quantum A Matter Of Size
- Quantum A Spooky Action at a Distance
- Quantum: A Walk Through the Universe
- Number of independent spatial modes in a spherical volume
- Quantum Computing Algorithms in the NISQ Era
- Quantum Formulas Collection
- Quantum Matter Elements and Particles
- Quantum mechanics

- Quantum optics beam splitter experiments
- Quantum: The Secret of Cohesion: How Waves Hold Matter Together
- Quantum Ultra fast lasers
- Template:Quantum optics operators
- Physical Sciences
- Phased array
- Orbital angular momentum of light
- 5D optical data storage

Notes

A. *Note: The calculations and limits below assume an ideal sphere, a homogeneous medium, and neglect losses, decoherence, or other non-ideal effects. An "independent mode" is defined here as an orthogonal spatial mode with minimal crosstalk*

B. *Note: Recent studies show that practical implementations of high-dimensional spatial modes can be limited by non-ideal media, optical aberrations, and detector limitations.*

C. *Note: Both polarizations are included in the count. The number N represents a theoretical limit; practically achievable values may be lower due to material imperfections or measurement errors.*

D. *Note: This geometric limit is theoretical; in practice, diffraction and interference can reduce the number of effectively usable beams.*

E. *Note: Although the total spatio-temporal modes increase with Δf·t, detector bandwidth, decoherence, and losses can limit the number of effectively measurable modes.*

F. *Note: This example gives a theoretical estimate (practical detection may yield far fewer modes than the theoretical (N_{total}).*

1. Miller, David A. B. (2000). "Communicating with waves between volumes: evaluating orthogonal spatial channels and limits on coupling strengths". *Applied Optics* **39** (11): 1681–1699. doi:10.1364/AO.39.001681.
2. Erhard, Manuel; Krenn, Mario; Zeilinger, Anton (2020). "Advances in high-dimensional quantum entanglement". *Nature Reviews Physics* **2**: 365–381. doi:10.1038/s42254-020-0193-5.
3. Fabre, Claude; Treps, Nicolas (2020). "Modes and states in quantum optics". *Reviews of Modern Physics* **92** (3). doi:10.1103/RevModPhys.92.035005.
4. Lloyd, Seth (2000). "Ultimate physical limits to computation". *Nature* **406**: 1047–1054. doi:10.1038/35023282.
5. Jensen, F. (1970). "The influence of inaccuracies of measurements on antenna near-field far-field correlation" (PDF). *Proc. Fourth Coll. on Microwave Communication*. Vol. III. Budapest. pp. ET-13.
6. Jensen, F. (1970). *Electromagnetic near-field far-field correlations* (Ph.D.). Lab. of Electromagnetic Theory, Technical University of Denmark. LD 15.
7. Yurchin, V.I.; Tseytlin, N.M. (1979). "Antenna testing based on near-field measurements (Review)". *Radio Engineering and Electronic Physics* **24** (12): 1–26. https://publications.rwth-aachen.de/record/815778/files/815778.pdf.
8. Hansen, J.E. (1988). *Spherical Near-Field Antenna Measurements*. London: Peter Peregrinus Ltd.. doi:10.1049/pbew026e. ISBN 978-0-86341-110-6. https://digital-library.theiet.org/content/books/ew/pbew026e.
9. Lemanczyk, J.; Jensen, F. (1991). "The calibration of probes for near-field measurements". *Proc. 13th Annual Meeting and Symposium Antenna Measurements Techniques Association (AMTA)*. Boulder, CO. pp. 9-5–9-10.
10. Dirix, Marc; Gregson, Stuart F.; Dubrovka, Rostyslav F. (2025-09-05). "Use of the Generalized Vector Addition Theorem for Antenna Position Translation for Spherical Mode-Filtering-Based Reflection Suppression". *Sensors* (MDPI) **25** (17). doi:10.3390/s25175557. PMID 40942983. PMC PMC12430979. https://www.ncbi.nlm.nih.gov/pmc/articles/PMC12430979/. Retrieved 2026-01-07.
11. Bucci, Ovidio M.; D'Elia, Giuseppe; Migliore, Marco Donald (2004). "A general and effective clutter filtering strategy in near-field antenna measurements". *IEE Proceedings - Microwaves, Antennas and Propagation* **151** (3): 227–235. doi:10.1049/ip-map:20040267.
12. Hindman, Greg E.; Newell, Allen C. (2005-10-30). *Reflection Suppression in a Large Spherical Near-Field Range*. Proceedings of the 27th Annual Meeting and Symposium of the Antenna Measurement Techniques Association (AMTA). Newport, RI, USA.
13. Hindman, Greg E.; Newell, Allen C. (2006-05-01). *Reflection Suppression to Improve Anechoic Chamber Performance*. Proceedings of the AMTA Europe. Munich, Germany.
14. Hess, Daniel W. (2007-11-11). *The IsoFilter™ Technique: Isolating an Individual Radiator from Spherical Near-Field Data Measured in a Contaminated Environment*. Proceedings of the EuCAP 2007. Edinburgh, UK.

Suppression in Cylindrical Near-Field Antenna Measurement Systems—Cylindrical MARS. Proceedings of the AMTA. Salt Lake City, UT, USA.

16. Parini, Clive G.; Gregson, Stuart F.; McCormick, John; van Rensburg, Daniël Janse; Eibert, Thomas (2021). *Theory and Practice of Modern Antenna Range Measurements: Volumes 1 & 2* (2nd ed.). Stevenage, UK: IET Press. ISBN 978-1-83953-126-2.
17. Newell, Allen C. (1988-06). "Error Analysis Techniques for Planar Near-Field Measurements". *IEEE Transactions on Antennas and Propagation* **36** (6): 754–768. doi:10.1109/8.1177.
18. Chen, Zhong; Gregson, Stuart F.; Wang, Yihong (2023-10-08). *Novel Application of Compressed Sensing in Cylindrical Mode Filtering for Far-Field Antenna Measurements*. Proceedings of the Antenna Measurement Techniques Association Annual Symposium. Seattle, WA, USA.

Sensing Technique in a Complex Electromagnetic Environment. Proceedings of the EuCAP. Stockholm, Sweden.

20. Jensen, Frank (1975). "On the probe compensation for near-field measurements on a sphere". *Archiv für Elektronik und Übertragungstechnik* **29**: 305–308.
21. Wacker, Peter F. (1974). "Near-field antenna measurements using a spherical scan: Efficient data reduction with probe correction". *IEE Conference Publication*. Conference on Precision Electromagnetic Measurements. Vol. 113. pp. 286–288.
22. Kerns, David M. (1981). *Plane-Wave Scattering-Matrix Theory of Antennas and Antenna-Antenna Interactions*. NBS Monograph. **162**. Boulder, CO, USA: National Bureau of Standards.
23. Larsen, Flemming Holm (1980). *Probe-Corrected Spherical Near-Field Antenna Measurements*. Department of Electromagnetic Systems (PhD thesis). Lyngby, Denmark: Technical University of Denmark.

Addition Theorem". *Journal of Electromagnetic Waves and Applications* **7** (5): 651–665. doi:10.1163/156939393X00552.

25. "§14.10 Zeros". *Digital Library of Mathematical Functions*. National Institute of Standards and Technology. Retrieved 2025-08-11.
26. Hansen, Jørgen E., ed (1988). *Spherical Near-Field Antenna Measurements*. London, UK: Peter Peregrinus Ltd.. ISBN 978-0863411106.
27. Balanis, Constantine A. (1989). *Advanced Engineering Electromagnetics*. Hoboken, NJ, USA: John Wiley & Sons, Inc.. ISBN 978-0-471-62194-2.
28. Jensen, Frank; Frandsen, Aksel (2004-10-17). *On the Number of Modes in Spherical Wave Expansions*. Proceedings of the Antenna Measurement Techniques Association, Annual Symposium. Atlanta, GA, USA.
29. Dirix, Marc (2018). *Quiet Zone Performance Qualification Using Spherical Near-Field Scanning*. Munich, Germany: Dr. Hut. ISBN 978-3-8439-3576-0.
30. "Altair Feko". *Altair*. Retrieved 2025-05-20.

Predication of Planar Near-Field Measurements Based on Full-Wave Three-Dimensional CEM Measurement Simulation. Proceedings of the AMTA. Seattle, WA, USA.

32. Chew, W. C. (2008). "Vector Addition Theorem and Its Diagonalization". *Communications in Computational Physics* **3** (2): 330–341. https://www.global-sci.com/index.php/cicp/article/download/5517/10971/12201.
33. J. D. Bekenstein, "Universal upper bound on the entropy-to-energy ratio for bounded systems", *Physical Review D* **23**, 287 (1981). DOI: 10.1103/PhysRevD.23.287 (https://doi.org/10.1103/PhysRevD.23.287)
34. Bousso, Raphael; Kaya, Sami (April 2025). "Holographic entropy cone beyond AdS/CFT". *Physical Review D* **111** (8): 086014. doi:10.1103/PhysRevD.111.086014. https://journals.aps.org/prd/abstract/10.1103/PhysRevD.111.086014.

Annual Meeting of the Antenna Measurement Techniques Association (AMTA). Stone Mountain Park, GA, USA. pp. 489–494.

36. Toraldo di Francia, G. (1969). "Degrees of freedom of an image". *Journal of the Optical Society of America* **59** (7): 799–804. doi:10.1364/JOSA.59.000799.
37. Lukosz, W. (1966). "Optical systems with resolving powers exceeding the classical limit". *Journal of the Optical Society of America* **56** (11): 1463–1472. doi:10.1364/JOSA.56.001463.
38. Dirix, Marc; Gregson, Stuart F.; Dubrovka, Rostyslav F. (5 September 2025). "Use of the Generalized Vector Addition Theorem for Antenna Position Translation for Spherical Mode-Filtering-Based Reflection Suppression". *Sensors* **25** (17): 5557. doi:10.3390/s25175557. https://www.mdpi.com/1424-8220/25/17/5557. Retrieved 8 February 2026.

Press. ISBN 978-0-521-48413-8.

40. Erhard, Manuel; Fickler, Robert; Krenn, Mario; Zeilinger, Anton (2017). "Twisted photons: new quantum perspectives in high dimensions". *Light: Science & Applications* **6** (10): e17146. doi:10.1038/lsa.2017.146. PMID 29138663. PMC 5655069. //www.ncbi.nlm.nih.gov/pmc/articles/PMC5655069/.
41. Conway, John H.; Sloane, Neil J. A. (1999). *Sphere Packings, Lattices and Groups* (3rd ed.). Springer. ISBN 978-0-387-98585-5.
42. Brecht, Bernd; Reddy, Divya V.; Silberhorn, Christoph; Raymer, Michael G. (2015). "Photon temporal modes: a complete framework for quantum information science". *Physical Review X* **5**: 041017. doi:10.1103/PhysRevX.5.041017.